Chiral Induction Effects in Ruthenium(II) Amino Alcohol Catalysed Asymmetric Transfer Hydrogenation of Ketones: An Experimental and Theoretical Approach

Daniëlle G. I. Petra,[a] Joost N. H. Reek,[a] Jan-Willem Handgraaf,[b] Evert Jan Meijer,[b] Peter Dierkes,[a] Paul C. J. Kamer,[a] Johannes Brussee,[c] Hans E. Schoemaker,[d] and Piet W. N. M. van Leeuwen*[a]

Abstract: The enantioselective outcome of transfer hydrogenation reactions that are catalysed by ruthenium(II) amino alcohol complexes was studied by means of a systematically varied series of ligands. It was found that both the substituent at the 1-position in the 2-amino-1-alcohol ligand and the substituent at the amine functionality influence the enantioselectivity of the reaction to a large extent: enantioselectivities (*ee* values) of up to 95% were obtained for the reduction of acetophenone. The catalytic cycle of ruthenium(II) amino alcohol catalysed transfer hydrogenation was examined at the density functional theory level. The formation of a hydrogen bond between the carbonyl functionality of the substrate and the amine proton of the ligand, as well as the formation of an intramolecular H···H bond and a planar H-Ru-N-H moiety are crucially important for the reaction mechanism. The enantioselective outcome of the reaction can be illustrated with the aid of molecular modelling by the visualisation of the steric interactions between the ketone and the ligand backbone in the ruthenium(II) catalysts.

Keywords: asymmetric catalysis · density functional calculations · hydrogen transfer · reaction mechanisms · ruthenium

Introduction

Asymmetric reduction of C=O and C=N bonds to chiral alcohols and amines, respectively, are amongst the most essential molecular transformations.[1] In order to be applicable for the industrial synthesis of fine chemicals and in organic laboratories, the synthesis of these compounds should be economically and technically feasible and should also have a broad scope. A reaction that uses non-hazardous organic molecules provides a very useful complement to catalytic reduction with molecular hydrogen, particularly for small- to medium-scale reactions. Transfer hydrogenation of ketones and imines is operationally simple and the selectivities, including functional group differentiation, are high. Among the most active catalysts for the asymmetric transfer hydrogenation of prochiral ketones are ruthenium(II) amino alcohol catalysts, as was reported by Noyori et al. and also further explored by others.[2–5]

Although the results are satisfactory in terms of activity and selectivity, the mechanism of the reaction has not been elucidated as yet. Two mechanistic pathways have been proposed for the asymmetric hydrogen-transfer reaction (Scheme 1): a stepwise process through a hydride complex (Path A) and a concerted process in which the hydrogen is directly transferred from the secondary alcohol to the substrate (Path B).[6]

For the ruthenium-catalysed transfer hydrogenation some key features have been discovered that support the hydridic route (Path A). Noyori and co-workers showed that the structure of the proposed active species in ruthenium(II)-catalysed transfer hydrogenation is a 16-electron ruthenium(II) complex that bears a TsDPEN ligand and an η^6-arene moiety (TsDPEN = *N*-(*p*-tolylsulfonyl)-1,2-diphenylethylenediamine).[7] In the presence of 2-propanol, an 18-electron *ruthenium hydride* species is formed that catalyses the reduction of various ketones. Furthermore, it was shown that the presence of an NH moiety in the ligand is of crucial

[a] Prof. P. W. N. M. van Leeuwen, Dr. D. G. I. Petra, Dr. J. N. H. Reek, Dr. P. Dierkes, Dr. P. C. J. Kamer
Institute of Molecular Chemistry, University of Amsterdam
Nieuwe Achtergracht 166, 1018 WV Amsterdam (The Netherlands)
Fax: (+31) 20-5256456
E-mail: kamer@anorg.chem.uva.nl, PWNM@anorg.chem.uva.nl

[b] J.-W. Handgraaf, Dr. E. J. Meijer
Department of Chemical Engineering, University of Amsterdam
Nieuwe Achtergracht 166, 1018 WV Amsterdam (The Netherlands)

[c] Dr. J. Brussee
Leiden Institute of Chemistry, Gorlaeus Laboratories
University of Leiden
P.O. Box 9502, 2300 RA Leiden (The Netherlands)

[d] Prof. H. E. Schoemaker
DSM Research
P.O. Box 18, 6160 MD, Geleen (The Netherlands)

  0947-6539/00/0615-2818 $ 17.50+.50/0

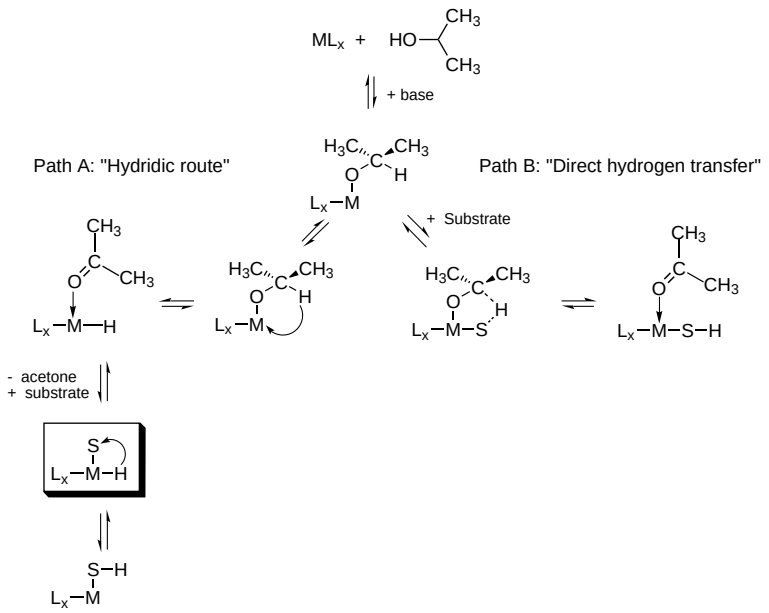

Scheme 1. Two mechanistic pathways for asymmetric transfer hydrogenation.

importance to obtain the product in high yield and enantiomeric excess. However, the precise process of the hydrogen transfer from the metal to the substrate, in the step which determines the enantioselectivity, is still unresolved (see box in Scheme 1).

Previously, we investigated possible factors that affect the enantioselectivity of hydrogen transfer reactions catalysed by ruthenium amino alcohol catalysts.[5] The preferred mode of ligand coordination and the effect of various substituents on the carbon backbone and on the amine functionality were studied.

It was found that the active catalyst contains one amino alcohol ligand which coordinates to the ruthenium atom in a bidentate fashion. These results are in agreement with those of Noyori and co-workers for the ruthenium(II)–TsDPEN system.[7] Our study resulted in the most effective chiral amino alcohol ligand for Ru^{II}-catalysed hydrogen transfer of various ketones so far (namely catalyst **12**, Table 1).

Herein we show that the crucial mechanistic step that determines the enantioselectivity of ruthenium(II)-catalysed transfer hydrogenation reactions is revealed by means of a combination of experimental and computational data. A systematic variation of the amino alcohol ligands allowed the determination of the relationship between the ligand structure and the enantioselectivity in the ruthenium(II)-catalysed transfer hydrogenation of acetophenone. The experimental data are supported by a theoretical study at the density functional level of theory. The actual process of the transfer of a hydride from the metal to the substrate was calculated. Based on the computed structures of various potential catalytic intermediates, a mechanism is proposed for the transfer hydrogenation catalysed by Ru^{II} amino alcohol complexes.

Results and Discussion

Experimental study: In order to elucidate the factors that determine the enantioselective outcome of the reaction, a series of amino alcohol ligands was used in the ruthenium(II)-catalysed transfer hydrogenation of acetophenone. A variation in the substituents of the amino alcohol ligand and the arene moiety allowed a systematic study of these factors. The general catalyst structure is given in Table 1.

The amino alcohols that contain an alkyl or aryl substituent at the *2-position* (as in **1** and **3**) are derived from naturally occurring amino acids, whereas amino alcohols that bear an aryl substituent at the *1-position* can only be obtained by means of a different synthetic strategy. The synthesis of the amino alcohols in **6**–**9** from the corresponding (*R*)-cyanohydrins, was reported previously.[8]

Table 1. Ruthenium(II) amino alcohol catalysts **1**–**14**.

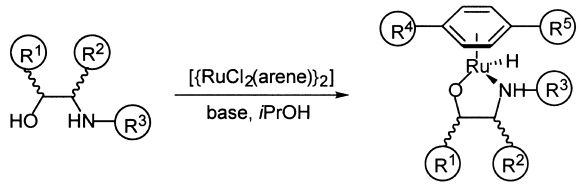

1-14

Catalyst	Amino alcohol configuration	R^1	R^2	R^3	R^4	R^5
1	2*S*	H	CH_3	H	H	H
2	1*S*	CH_3	H	H	H	H
3	2*S*	H	CH_3	H	CH_3	*i*Pr
4	1*S*	CH_3	H	H	CH_3	*i*Pr
5	2*R*	H	Ph	H	CH_3	*i*Pr
6	1*R*	*p*-OMe-Ph	H	H	CH_3	*i*Pr
7	1*R*	*p*-OMe-Ph	H	CH_3	CH_3	*i*Pr
8	1*R*	Ph	H	CH_3	CH_3	*i*Pr
9	1*R*	Ph	H	*i*Pr	CH_3	*i*Pr
10	1*R*,2*S*	Ph	CH_3	H	CH_3	*i*Pr
11	1*R*,2*S*	Ph	CH_3	CH_3	CH_3	*i*Pr
12	1*R*,2*S*	Ph	CH_3	CH_2-Ph	CH_3	*i*Pr
13	1*R*,2*S*	Ph	CH_3	CH_3	H	H
14	1*R*,2*S*	Ph	CH_3	CH_2-Ph	H	H

The in situ generated catalysts **1**–**14** were used in the reduction of acetophenone (Scheme 2, Table 2).

In a typical catalysis experiment, a solution of ketone (0.1M in dry 2-propanol), the ruthenium complex ([{$RuCl_2$(arene)}$_2$], 0.25 mol%), the chiral amino alcohol (0.6 mol%) and *t*BuOK (1.5 mol%) were stirred at room temperature under argon in dry 2-propanol. Conversions and enantiose-

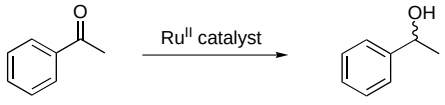

Scheme 2. Asymmetric transfer hydrogenation of acetophenone.

  0947-6539/00/0615-2819 $ 17.50+.50/0

Table 2. Hydrogen transfer reduction of acetophenone with catalysts **1**–**4**.[a]

Entry	Catalyst	t [h]	Conversion [%][b]	ee [%][c]	Configuration	$\Delta(\Delta G^{\neq})$ [kcal mol^{-1}][e]
1	**1**	1	93	6	(*S*)	0.07
2	**2**	1	90	52	(*S*)	0.67
3	**3**	1	88	15	(*S*)	0.18
4	**4**	1	84	63	(*S*)	0.86
5	**5**	1	85	24	(*R*)	0.29
6	**6**	1	89	61	(*R*)	0.83
7	**7**	1	91	76	(*R*)	1.16
8	**8**	1	93	75	(*R*)	1.13
9	**9**	1	94	84	(*R*)	1.42
10[d]	**10**	0.5	95	77	(*R*)	1.19
11[d]	**11**	0.5	91	89	(*R*)	1.66
12[d]	**12**	1	88	95	(*R*)	2.13
13	**13**	1	86	58	(*R*)	0.77
14	**14**	1	94	72	(*R*)	1.06

[a] The reaction was carried out at 20 °C with 5 mmol substrate in a 0.1 M 2-propanol solution; substrate:[{RuCl(arene)$_2$}$_2$]:ligand:*t*BuOK = 400:1:2.2:3.3. [b] Conversions were determined by GLC analysis. [c] Determined by capillary GLC analysis on a chiral cycloSil-B column. [d] This data was obtained from Ref. [5]. [e] $\Delta(\Delta G^{\neq})$ values are calculated from the *ee* values: $\Delta(\Delta G^{\neq}) = RT \ln K$; $K = (100 - x)/x$; $x = (100 - ee)/2$.

lectivities were monitored during the reaction by GC. The enantioselectivity proved to be constant in time for all catalytic reactions described. The reaction rates were relatively constant with various amino alcohol ligands and gave rise to high conversions (≈90 %) after 1 h at room temperature.

The difference in chiral induction by the use of either *1-* or *2-substituted* amino alcohol ligands in the reduction of acetophenone was investigated with the most simple catalysts, namely, **1** and **2**. The use of **1** as the catalyst gave rise to a very low enantioselectivity of 6 % (Table 2, entry 1), while the observed enantioselectivity was significantly higher with **2**, namely 52 % (Table 2, entry 2). In order to be able to compare differences in enantioselectivities on a linear scale, the enantioselectivities of the reactions were quantified by calculating from the observed *ee* values the differences in the Gibbs free energy of activation for the (*R*) or the (*S*) product (Table 2). The difference in enantioselectivity between catalyst **1**, that contains a *2-substituted* amino alcohol, and catalyst **2**, that contains a *1-substituted* amino alcohol, corresponds to a difference in $\Delta(\Delta G^{\neq})$ of 0.6 kcal mol^{-1}.

The use of the ruthenium *p*-cymene complex as a catalyst precursor gave rise to higher enantioselectivities than the benzene-substituted catalyst (Table 2, entries 3 and 4). This increase in enantioselectivity, which corresponds to a difference of $\Delta(\Delta G^{\neq}) = 0.2$ kcal mol^{-1}, has been observed in most other systems as well and is proposed to be caused by increased steric bulk.[2, 3, 5] With the (*p*-cymene)ruthenium(II) chloride dimer, the enantioselection of the 1- and 2-substituted amino alcohol ligands were similar, corresponding to a difference in $\Delta(\Delta G^{\neq})$ of 0.7 kcal mol^{-1}.

The difference between various R^2 substituents was investigated by the use of the *2-substituted*, naturally occurring amino alcohols (*R*)-alaninol (in **3**) and (*R*)-2-phenyl glycinol (in **5**) as ligands in ruthenium-catalysed transfer hydrogenation. When the steric bulk at the 2-position was increased, with **5** as a catalyst, the observed enantioselectivity was somewhat higher compared to the methyl-substituted **3** (24 % versus 15 %, Table 2, entries 3 and 5). Even when large R_2 substituents were employed, only poor enantioselectivities could be obtained, corresponding to a small $\Delta(\Delta G^{\neq})$ of 0.3 kcal mol^{-1}.

The use of catalysts that contain different R^1 substituents was investigated with *1-substituted* amino alcohols, which generally resulted in higher enantioselectivities. Surprisingly, the more bulky *p*-methoxyphenyl substituent (in **6**) did not give rise to higher enantioselectivities than the relatively small methyl group (in **4**) (Table 2, entries 4 and 6). Hence, a very small chiral ligand ($R^1 = CH_3$) already suffices for the reduction of acetophenone with an enantioselectivity of more than 60 %. This suggests that $\pi-\pi$ stacking between the substrate and the amino alcohol ligand is of minor importance. By variation of the R^1 substituents good enantioselectivities could be obtained, corresponding to differences in $\Delta(\Delta G^{\neq})$ of up to 0.8 kcal mol^{-1}. Optimisation of the ligand structure to obtain higher enantioselectivities was accomplished by varying the R^2–R^5 substituents.

The difference between various R^3 substituents on the nitrogen atom was investigated by the use of the *amine-substituted* catalysts **7**–**9**. Catalyst **7**, which contains a secondary amine ($R^3 = CH_3$) gave rise to a higher enantioselectivity than the corresponding primary amine in **6** ($R^3 = H$), namely 76 and 61 %, respectively (Table 2, entries 6 and 7). The corresponding difference in $\Delta(\Delta G^{\neq})$ is 0.3 kcal mol^{-1}. A similar enantioselectivity was obtained with catalyst **8** ($R^3 = CH_3$) which contains a phenyl group instead of a *p*-methoxyphenyl group at the 1 position (Table 2, entry 8). The change of R^3 from a methyl (in **8**) to an isopropyl group (in **9**) caused the enantioselectivity to increase further from 74 to 84 % and the corresponding $\Delta(\Delta G^{\neq})$ to increase from 1.13 to 1.42 kcal mol^{-1} (Table 2, entries 8 and 9). Thus, substitution of the amine functionality results in higher enantioselectivities than those obtained for the corresponding unsubstituted amino alcohols. Differences in $\Delta(\Delta G^{\neq})$ of 0.6 kcal mol^{-1} or less could be reached upon changing $R^3 = H$ into $R^3 = i$Pr.

The effect of an additional substituent at the 2 position was studied with *1,2-disubstituted* amino alcohols as ligands. The use of (1*R*,2*S*)-(nor)ephedrine (in **10** and **11**) resulted in an increase in enantioselectivity compared to **6** and **7** (Table 2, entries 10 and 11). The product configuration did not change on when these 1,2-disubstituted amino alcohols were employed. Noyori and co-workers showed that the use of (1*S*, 2*R*)-ephedrine and (1*S*, 2*S*)-pseudoephedrine in [{Ru(C_6-Me_6)Cl_2}$_2$]-catalysed transfer hydrogenation gave rise to identical enantioselectivities and the same product configuration.[2] Thus, the increase in the enantioselectivities, caused by the additional methyl substituent at the 2 position, is more accurately described as an overall increase in the steric hindrance rather than a chiral cooperativity effect. The use of (1*R*,2*S*)-*N*-benzyl-norephedrine (in **12**), developed previously, proved to be the best amino alcohol ligand so far; it gave 95 % *ee* and 88 % conversion in one hour for the ruthenium(II)-catalysed transfer hydrogenation of acetophenone (Table 2, entry 12). Thus, the additional substituent at the 2-position gave rise to higher enantioselectivities than the

  0947-6539/00/0615-2820 $ 17.50+.50/0 *Chem. Eur. J.* **2000**, *6*, No. 15

corresponding unsubstituted ligands to result in additional differences in $\Delta(\Delta G^{\neq})$ of 0.5 kcal mol^{-1} or less. Furthermore, changing the R^3 substituent in the last series of ligands (**10**–**12**) from $R^3 = H$ to $R^3 = Bn$ increased the differences in $\Delta(\Delta G^{\neq})$ of up to 1.0 kcal mol^{-1}, to result in a $\Delta(\Delta G^{\neq})$ of 2.13 kcal mol^{-1}.

The use of the two best amino alcohol ligands, (1*R*,2*S*)-ephedrine and (1*R*,2*S*)-*NH*-benzyl-norephedrine, in combination with the (benzene)ruthenium(II) chloride dimer, as in **13** and **14** (R^4 and $R^5 = H$), gave rise to much lower enantioselectivities (namely 58 and 72%, respectively) than the corresponding *p*-cymene-substituted complexes (89 and 95%, respectively) (Table 2, entries 13 and 14). In this case, differences in $\Delta(\Delta G^{\neq})$ of up to 0.9 kcal mol^{-1} were obtained. This is a much larger decrease than the differences between the benzene-substituted catalysts **1** and **2** and the *p*-cymene-substituted catalysts **3** and **4**. Apparently, additional steric interactions between the R^4 and R^5 substituents on the arene and the R^3 substituent on the nitrogen atom gives rise to further improvement of the enantioselective outcome of the reaction. Thus, a highly substituted framework around the metal atom results in fewer degrees of freedom and consequently in higher enantioselectivities.

In summary, the catalysis results presented in Table 2 show that the product configuration is determined by the substituent at the 1-position in the amino alcohol ligand, and gives rise to differences in $\Delta(\Delta G^{\neq})$ of up to 0.6 kcal mol^{-1}. This chiral centre highly affects the enantioselective outcome of the reaction. Remarkably, no difference was observed in the use of either small or large groups at this position. Optimisation of the ligand structure is most effective at the R^3, R^4 and R^5 positions to result in large improvements of the enantioselectivities; the observed $\Delta(\Delta G^{\neq})$s are 1.0 kcal mol^{-1} or less. Additional substitution at the R^2 position further improves the enantioselectivity to give $\Delta(\Delta G^{\neq})$s that increase up to 0.5 kcal mol^{-1}. The three-dimensional steric bulk around the metal atom, created by the substitutents at several positions on the ligands, is essential to obtain high asymmetric inductions.

Possible ways to transfer a hydride: In order to get more insight in the results described above, especially in the marked differences in chiral induction that were found in the use of the 1- versus 2-substituted amino alcohols as ligands in the ruthenium-catalysed reduction of acetophenone, a closer look at the step which determines the enantioselectivity is required. Scheme 3 shows the two possible ways in which a hydride can be transferred from the metal to the substrate. Route I visualises the general six-membered cyclic transition structure proposed by Noyori and co-workers.[9, 10] From this it is obvious that the proton in the amine functionality plays a crucial role by the formation of a hydrogen bond to the carbonyl oxygen.

As an alternative pathway, Bäckvall and co-workers reported on a migratory insertion-type of mechanism for ruthenium(II)-catalysed transfer hydrogenation with [$RuCl_2(PPh_3)_3$] as a catalyst precursor.[11] Here, the substrate coordinates through the π system of the carbonyl functionality to the ruthenium catalyst in the enantioselectivity determining step. The analogous transition structure for [RuH(arene)(amino alcohol)] is depicted in Route II, Scheme 3.

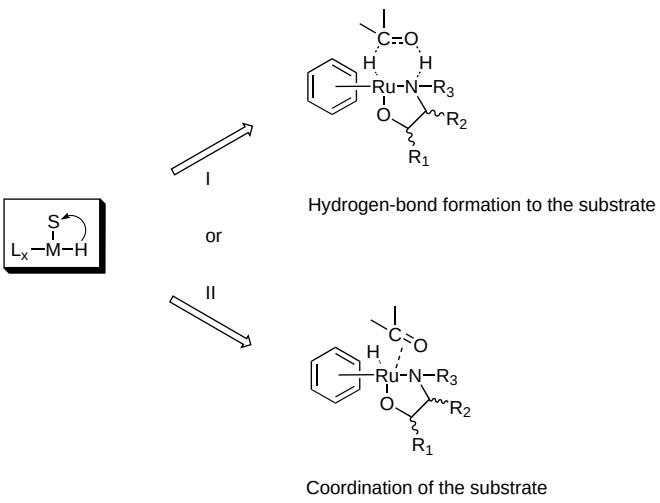

Scheme 3. Possible ways to transfer a hydride.

In order to distinguish between these two routes (i.e. I versus II) the ruthenium amino alcohol complexes of the two catalytic cycles were investigated theoretically at the density functional theory (DFT) level.

Theoretical study: Ruthenium hydride complexes have been studied extensively at the density functional theory (DFT) level.[12]-[15] The relative stabilities of various ruthenium hydride complexes which bear phosphorus ligands have been calculated with either B3LYP or B3PW91 as the hybrid functionals. These studies proved that the role of intermolecular H···H bonding is important in proton-transfer reactions.

Here we describe an investigation on ruthenium hydride complexes that contain an amino alcohol ligand and an arene moiety. In the calculations, the amino alcohol ligand was initially modelled by an NH_3 and a deprotonated H_2O ligand, whereas the hydrogen donor and acceptor were modelled by methanol and formaldehyde, respectively. Benzene was chosen as the arene moiety.

Methods of calculation: The electronic structure was computed within the Kohn–Sham formulation of DFT by means of the gradient-corrected local functionals. We performed initial calculations with a medium-sized basis set with the Gaussian package.[16] These results served as input for more extensive calculations with a larger basis set which were performed with the ADF package.[17, 18] We performed calculations with the B3PW91 functional and the Gaussian 98 package. This functional consists of Becke's three-parameter hybrid-functional for exchange [27] combined with a gradient-corrected correlation term, as proposed by Perdew and Wang.[20] The Gaussian calculations were performed with the LANL2DZ double ζ basis set.[21, 22] We then performed calculations with the PW91 and BLYP functional with the ADF package. Here, PW91 refers to the LDA functional with the VWN parameterisation[23] complemented with a gradient correction for exchange and correlation proposed by Perdew and Wang.[20] The BLYP density functional consists of the

gradient-corrected exchange term proposed by Becke[19] together with a correlation term proposed by Lee, Yang and Parr.[24] The ADF calculations were performed with a large basis set.[26]

It has been shown by comparative analysis of transition-metal hydride complexes that BLYP, B3LYP and B3PW91 give qualitatively similar results.[14, 15, 28, 33] However, as has been shown by Orlova et al., for the special case of intermolecular hydrogen-bonded transition metal complexes, the B3PW91 geometries and bond energies are in better overall agreement with the experimental data.[14, 29]

Comparison of the proposed mechanisms: Two different catalytic cycles are proposed for hydrogen-transfer reactions. The "hydrogen-bond formation" mechanism for ruthenium-catalysed transfer hydrogenation is depicted in Scheme 4, and the "migratory insertion" mechanism for ruthenium(II) amino alcohol catalysed transfer hydrogenation is shown in Scheme 5.

The d^6 complexes [RuH(benzene)(NH_3)(OH)] are models for the supposed [RuH(benzene)(amino alcohol)] complexes. On account of the structural similarities between the hydrogendonor and the product alcohol, the reduction of acetophenone in 2-propanol is close to a thermodynamic equilibrium.[10] Therefore, each step in the catalytic cycle should be reversible and the catalytic cycle and the corresponding energy profile should be symmetrical.

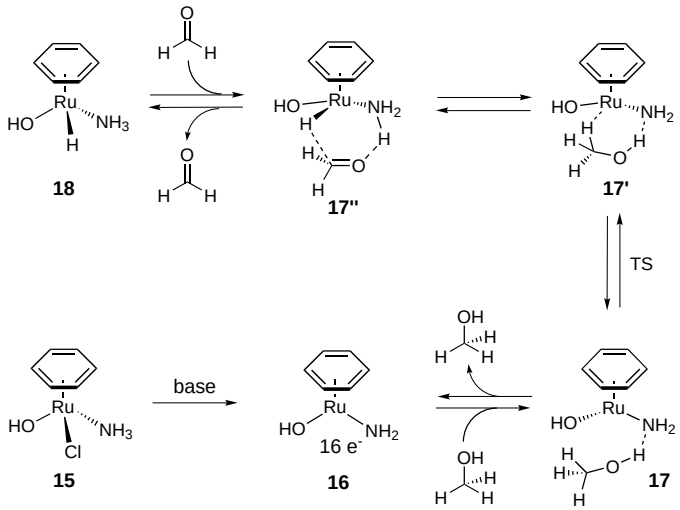

Scheme 4. The "hydrogen-bond formation" mechanism.

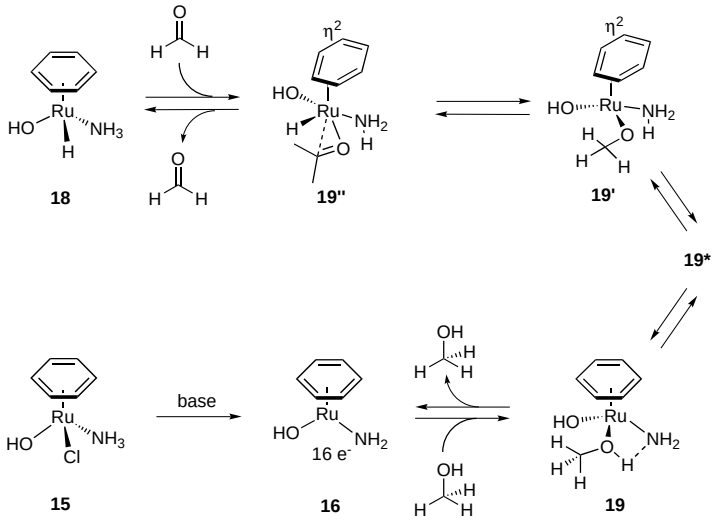

Scheme 5. The "migratory insertion" mechanism.

A geometry optimisation has been performed on intermediates **16**–**18**, formaldehyde, and methanol with the different functionals described above. The relative energies of the geometries and the corresponding energy profile, calculated by the use of the PW91 functional, are depicted in Figure 1. The calculated B3PW91 and PW91 relative energies and distances of intermediates **16**–**18** are given in Table 3. All the intermediates of the cycle depicted in Figure 1 were calculated to have relative energies between 0 and 15.4 kcal mol^{-1}. The B3PW91 and PW91 functionals gave rise to similar results. In addition, single-point calculations with the BLYP functional resulted in a comparable trend in the relative energies with differences of up to 1.5 kcal mol^{-1}.

The unsaturated 16-electron species **16** is formed under basic conditions starting from complex **15.** In complex **16** the calculated Ru–N bond length is somewhat shorter than that in the other intermediates, which indicates a stronger bond between the ruthenium and the nitrogen atom. This is also observed in the crystal structures of the analogous complexes of **15**, **16** and **18** reported by Noyori and co-workers.[7] In the presence of an alcoholic solvent, the ruthenium hydride complex **18** is formed spontaneously and the corresponding carbonyl compound is released.

Reduction of the ketone substrate, modelled by formaldehyde, occurs by transfer of a proton and a hydride from complex **18** to the carbonyl compound, in several steps, as is visualised in Scheme 4 and Figure 1. A hydrogen bond between the lone pair electrons of the oxygen of the carbonyl and the amine proton is formed, as is calculated for **17″**. The calculated relative energy of **17″** is lower than that of complex **18** and formaldehyde separately, because of the formation of the hydrogen bond.[34] The C=O···H distance is 2.1 Å, which is short enough for a hydrogen bond to be formed, whereas the Ru–H···C=O distance is still 3.0 Å. The intramolecular H···H distance between ruthenium hydride and the proton of the amine functionality is small and thus provides additional stabilisation of the intermediates in the catalytic cycle (Table 3).

The next calculated intermediate, **17′**, not only shows a smaller C=O···H distance, namely 1.6 Å, but the ruthenium hydride is also at a very short distance from the carbonyl carbon atom (1.3 Å). The C=O bond is somewhat longer which indicates a decrease in the double-bond character. The relevant bond lengths of the calculated intermediates are given in Table 3.

The ADF package was used to calculate the transition state with the PW91 functional and resulted in intermediate **17**-TS. In **17**-TS the C–O bond length lies between that of methanol and methanal, namely 1.34 Å. The calculated C–O bond lengths for methanol and methanal are given in Table 4 for comparison.

In **17**-TS the ruthenium hydride distance has become 2.0 Å, the C–O···H distance has decreased to 1.3 Å and the O–C···H distance has become 1.2 Å. The carbonyl moiety and the intramolecular H···H bond prefer a coplanar relationship;

0947-6539/00/0615-2822 $ 17.50+.50/0 *Chem. Eur. J.* **2000**, *6*, No. 15

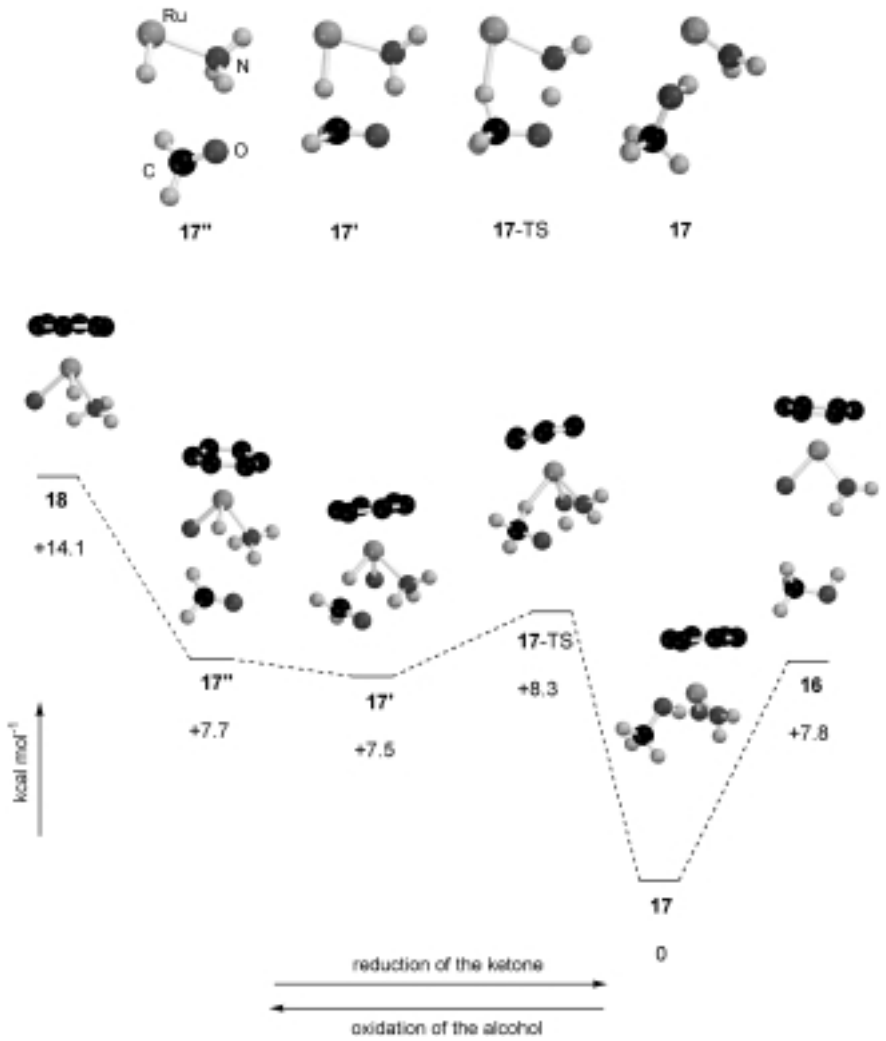

Figure 1. Energy profile for the "hydrogen-bond formation" mechanism. Non-relevant hydrogen atoms have been omitted for clarity.

Table 3. Calculated relative energies [kcal mol^{-1}] and distances [Å] in intermediates **16**–**18**.

Intermediate	Functional	ΔE	Ru–H	Ru–N	H···H	(C)O···H	(O)C···H	N···H	C···O
16	B3PW91[a]	+8.3	–	1.90	–	–	–	–	–
16	PW91[b]	+7.8	–	1.94	–	–	–	–	–
17	B3PW91[a]	0	5.09	1.94	2.44	1.00	1.10	1.90	1.44
17	PW91[b]	0	4.69	1.97	2.35	0.99	1.10	1.96	1.42
17-TS	PW91[b]	+8.3	1.97	2.08	2.06	1.26	1.19	1.23	1.34
17′	B3PW91[a]	+12.0	1.73	2.09	2.18	1.59	1.34	1.07	1.32
17′	PW91[b]	+7.5	1.76	2.13	2.17	1.64	1.34	1.07	1.28
17″	B3PW91[a]	+8.0	1.57	2.12	2.36	2.02	2.91	1.03	1.25
17″	PW91[b]	+7.7	1.60	2.17	2.41	2.07	2.97	1.03	1.22
18	B3PW91[a]	+15.4	1.59	2.13	2.47	–	–	–	–
18	PW91[b]	+14.1	1.61	2.17	2.53	–	–	–	–

[a] The B3PW91 results were obtained with the Gaussian 98 program and a double ζ basis set.[25] [b] The PW91 results were obtained with the ADF program and a triple ζ basis set.[26]

the dihedral H-Ru-N-H angle is as low as -13.0° in the transition state. Intermediate **17**, which is basically complex **16** with a methanol species hydrogen-bonded to the NH_2, is relatively low in energy. The release of the product alcohol results in the 16-electron complex **16**. The ruthenium hydride complex **18** is then formed according to the reverse order of steps as described in the foregoing text.

In summary, the results of these calculations support the "hydrogen-bond formation" mechanism in which the formation of a hydrogen bond between a proton of the amine functionality and the carbonyl of the ketone substrate is of crucial importance.

The other possible mechanism for ruthenium-catalysed transfer hydrogenation, the "migratory insertion" mechanism, is depicted in Scheme 5. Intermediates **16** and **18** are identical in both catalytic cycles. A geometry optimisation has been performed on intermediates **19**, **19***, **19′** and **19″**. The coordination of the ketone substrate in **19″** is in analogy to the $[RuH_2(PH_3)_3$(formaldehyde)] complex proposed by Bäckvall and co-workers.[11]

Since both functionals proved to be very consistent for the calculation of intermediates **16**–**18**, the intermediates **19**, **19***, **19′**, **19″**, were only calculated with PW91 by means of the ADF package. The relative energies of the geometries and the corresponding energy profile are depicted in Figure 2. The geometries of the η^6-C_6H_6 analogues of intermediates **19″**, **19′** and **19*** could not be optimised with the ADF package. The calculated η^4-C_6H_6 analogues of the intermediates were all higher in energy, for example, +24.6 kcal mol^{-1} for **19″**-η^4-C_6H_6 compared to +0.9 kcal mol^{-1} for **19″**-η^2-C_6H_6.

It can be seen from Table 5 that the calculated relative energies for most intermediates of the "migratory insertion" mechanism are in the same range as those of the analogous structures of the "hydrogen-bond formation" mechanism. This not the case for intermediate **19***-η^2, which has a calculated energy of +34.1 kcal mol^{-1}.

The ketone has to coordinate to the ruthenium in **18** through its π system in order to form intermediate **19″**. At the same time, the aromatic ring changes from an η^6 to an η^2 coordination. In the next calculated intermediate, **19′**-η^2-C_6H_6, the hydride has been transferred to the carbon atom of

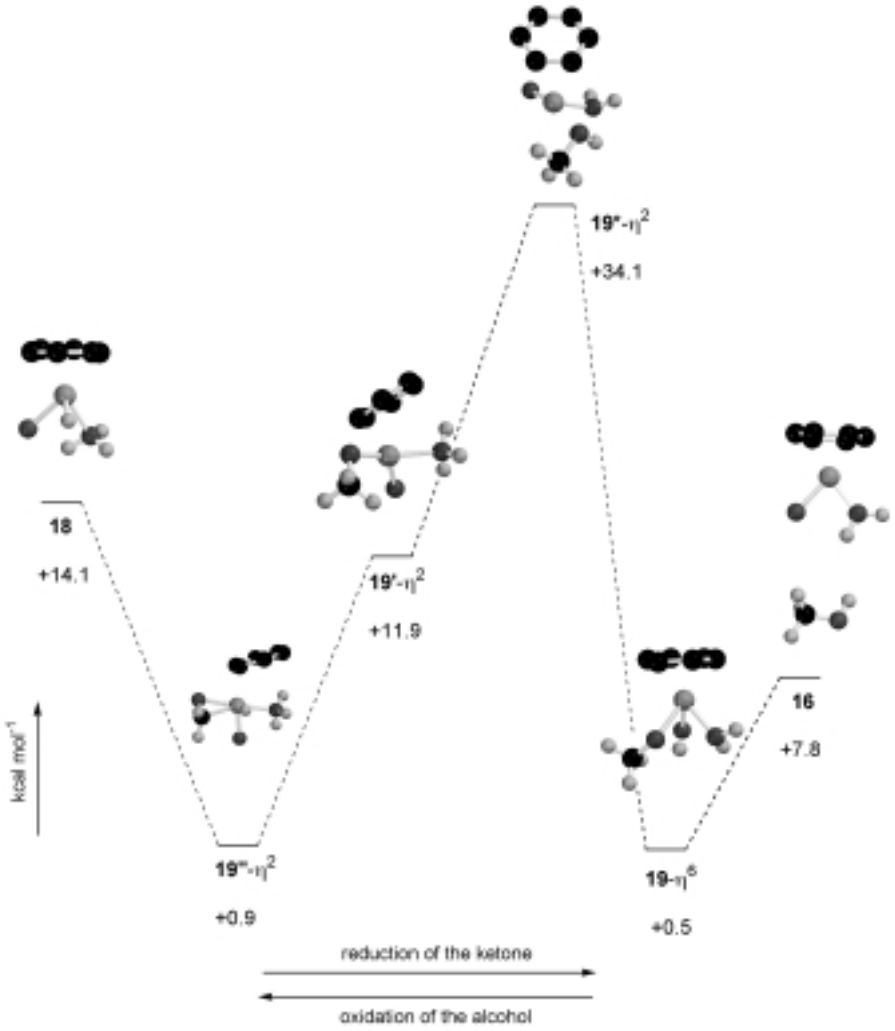

Figure 2. Energy profile for the "migratory insertion" mechanism. Non-relevant hydrogen atoms have been omitted for clarity.

Table 4. Calculated C–O distances [Å] in methanol and formaldehyde.

Molecule	Functional	Distance
CH_3OH	B3PW91[a]	1.45
CH_3OH	PW91[b]	1.43
H(CO)H	B3PW91[a]	1.24
H(CO)H	PW91[b]	1.21

[a] The B3PW91 results were obtained with the Gaussian 98 program and a double ζ basis set.[25] [b] The PW91 results were obtained with the ADF program and a triple ζ basis set.[26]

the ketone; this is obvious from the shorter distance to the carbonyl, namely 1.10 Å, and the longer Ru–H distance (2.65 Å). Furthermore, the C=O bond is longer which indicates a decrease in the double-bond character.

In the next step, the proton of the amine has been transferred to the coordinated oxygen, which makes the ruthenium atom more electron poor, as is shown by the calculations. This probably gives rise to the very high (+34.1 kcal mol^{-1}) relative energy of intermediate **19***-η^2-C_6H_6, which is not even a calculated transition state. In **19***-η^2-C_6H_6, the CO–H distance decreases to 0.98 Å and the N–H distance becomes 2.10 Å. This indicates that the proton transfer indeed has taken place. The length of the Ru–N bond is 0.19 Å shorter than that in **19′**-η^2-C_6H_6, which suggests a stronger bond between the ligand and the metal. In the next intermediates, the aromatic ring changed from an η^2 to an η^6 coordination and the alcohol dissociates from the complex.

The high relative energy of intermediate **19***-η^2 suggests that the "migratory insertion" path is less favourable than the "hydrogen-bond formation" mechanism. We have attempted to calculate several alternative pathways to find a migratory insertion mechanism with a lower energy barrier. The only mechanism found that was a low-energy process was assisted by coordination of a second alcohol to **19′**-η^2.[35] This resulted in an "alternative migratory insertion mechanism" as depicted in Scheme 6 and Figure 3. After the coordination of this second alcohol the energy is lower: 4.3 kcal mol^{-1} was found for **20**-η^2 (Table 5). The next step involves the transfer of a proton from the coordinated alcohol to the reduced ketone (i.e. OCH_3) to give intermediate **20′**-η^2. This proton is transferred with a very low energy barrier; the transition state, **20-TS-**η^2 , was calculated to have an energy of 7.8 kcal mol^{-1}. In this transition state the proton is, as expected, located between the oxygen atoms of the two coordinated methoxy groups. Although this alternative migratory insertion mechanism is a process with a low energy barrier, it is not in agreement with the experimental data obtained from a mechanistic study performed by Noyori et al.[7] They showed that both their analogues of structures **18** and **16** are intermediates in the reaction. Furthermore, at low concentrations of acetone, the reaction was first order in acetone and zero order in 2-propanol, and at low concentrations of 2-propanol the kinetics showed the reverse. In the alternative migratory insertion mechanism a higher order in 2-propanol is expected. Another strong argument against this mechanism is the necessity of a NH functionality in the ligand to obtain reasonable activity and selectivity. The NH group is not involved in the alternative migratory insertion mechanism. Also, not all transition states have been calculated yet, and we expect that the transition state between **18** and **19″**-η^2 is high in energy since the coordination mode of the aromatic ring changes from η^6 to η^2. All attempts to locate this transition state, however, failed.

0947-6539/00/0615-2824 $ 17.50+.50/0 *Chem. Eur. J.* **2000**, *6*, No. 15

Table 5. Calculated relative energies [kcal mol^{-1}] and distances [Å] in intermediates **19**, **19′**, **19″**, **20**, **20-TS** and **20′**[a]

Intermediate	ΔE	Ru–H	Ru–N	H···H	(C)O···H	(O)C···H	N···H	C···O
19-η^6	+0.5	3.17	2.10	2.45	1.05	1.10	1.57	1.43
19-η^4	+15.2	3.14	2.14	3.58	2.16	1.10	1.03	1.40
19*-η^2	+34.1	3.24	2.00	2.32	0.98	1.10	2.10	1.44
19′-η^2	+11.9	2.65	2.19	4.13	4.34	1.11	1.02	1.41
19″-η^4	+24.6	1.88	2.21	3.19	4.01	2.88	1.02	1.29
19″-η^2	+0.9	1.57	2.15	2.39	4.78	2.37	1.02	1.30
Intermediate	ΔE	C1–O	Ru–N	C2–O	Ru–OC1	Ru–OC2	H–OC1	H–OC2
20-η^2	+4.3	1.37	2.12	1.43	2.16	2.27	1.70	1.01
20-TS-η^2	+7.8	1.41	2.08	1.41	2.24	2.14	1.17	1.29
20′-η^2	+1.8	1.43	2.05	1.41	2.33	2.03	1.01	1.64

[a] The PW91 results were obtained with the ADF program and a triple ζ basis set.[26]

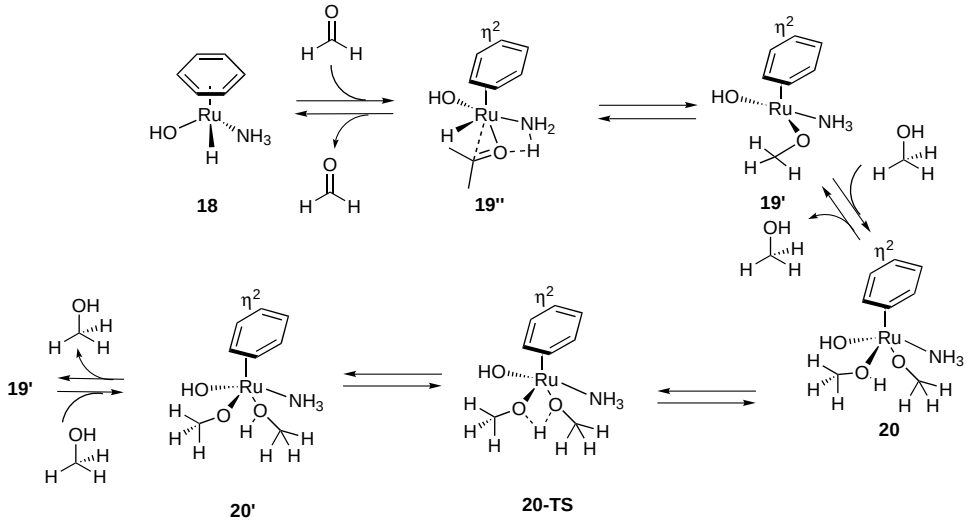

Scheme 6. The "alternative migratory insertion" mechanism.

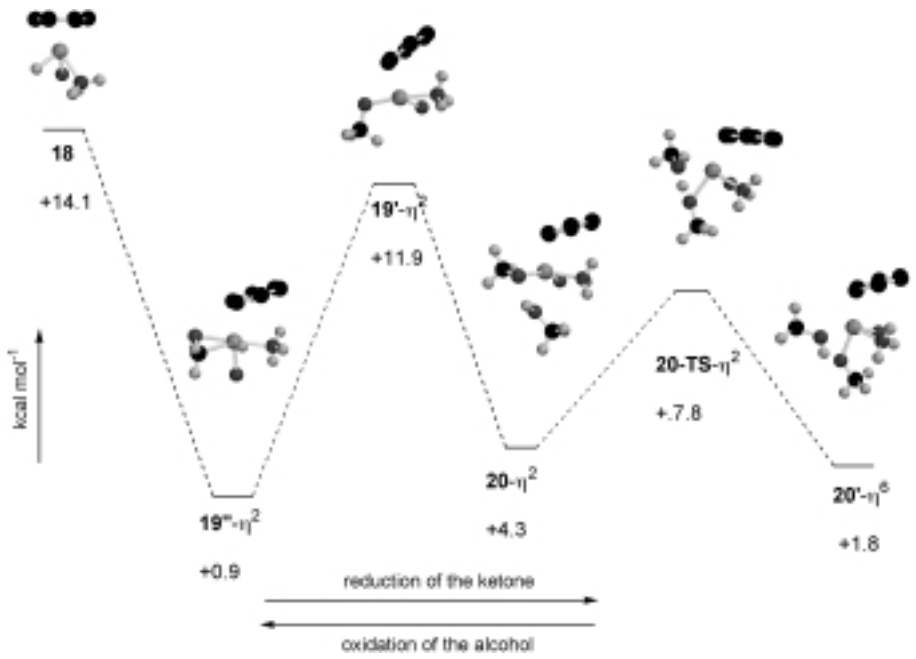

Figure 3. Energy profile for the "alternative migratory insertion" mechanism. Non-relevant hydrogen atoms have been omitted for clarity.

In conclusion, comparison of the two proposed mechanisms by DFT calculations of the possible intermediates that are involved shows that the "hydrogen-bond formation" mechanism is the pathway of choice for the transfer of the ruthenium hydride to the ketone substrate. The energy of the calculated intermediate **19***-η^2 is very high which makes the barrier much larger for the reaction path of the "migratory insertion" mechanism compared to the "hydrogen-bond formation" mechanism. In an "alternative migratory insertion" mechanism this barrier was calculated to be in the same range as that of the hydrogen bond mechanism; however, this proposed mechanism is not in agreement with the experimental data. The importance of the formation of a hydrogen bond between the proton of the amine functionality and the carbonyl of the ketone substrate is clearly shown in the "hydrogen-bond formation" mechanism. Furthermore, a small intramolecular H···H distance combined with a small H-Ru-N-H dihedral angle results in additional stabilisation. This dihedral is also small (-13°) in the calculated transition state.

*Ruthenium hydride complexes **1** and **2***: As was shown in the experimental study, a marked difference in chiral induction was found by the use of catalysts **1** and **2** in the asymmetric transfer hydrogenation of acetophenone. The geometries of ruthenium(II) amino alcohol hydride complexes **1** and **2** were optimised with the B3PW91 functional by the Gaussian package[26] to investigate the differences in the geometries. The calculated relative energies, bond lengths and dihedral angles are given in Table 6.

For each of these complexes two different ring conformations were found, as can be

Table 6. Calculated relative energies [kcal mol^{-1}], distances [Å] and dihedral angles (H-Ru-N-H and N-C2-C1-O) [°] in complexes **1** and **2**[a]

Complex	ΔE	Ru-H	Ru-N	Ru-O	(N)H · H·	H-Ru-N-H	N-C2-C1-O
(R_{Ru},S_C)-**1**-λ	+2.0	1.59	2.16	2.03	2.30	+23.4	−52.4
(R_{Ru},S_C)-**1**-δ	+3.8	1.58	2.13	2.04	2.60	+58.0	+47.7
(S_{Ru},S_C)-**1**-λ	+5.1	1.58	2.14	2.05	2.52	−46.8	−52.7
(S_{Ru},S_C)-**1**-δ	+1.4	1.59	2.15	2.03	2.30	−22.0	+51.9
(R_{Ru},S_C)-**2**-λ	+1.9	1.58	2.15	2.03	2.30	+17.0	−50.0
(R_{Ru},S_C)-**2**-δ	+2.5	1.58	2.13	2.04	2.57	+55.6	+49.1
(S_{Ru},S_C)-**2**-λ	+3.7	1.58	2.13	2.04	2.60	−58.2	−44.8
(S_{Ru},S_C)-**2**-δ	0	1.59	2.16	2.02	2.31	−24.5	+51.4

[a] The B3PW91 results were obtained with the Gaussian 98 program and a double ζ basis set.[26]

seen from the dihedral angles, N-C_2-C_1-O, in Table 6. The puckered five-membered chelate ring is a chiral entity.[36, 37] The chirality of a given ring conformation is defined by considering two skewed lines, the line connecting the N and O atoms and the C–C bond, as axis and tangent of a helix, the right- and left-handedness of which is designated δ and λ. The δ and λ ring conformations of a general ruthenium amino alcohol complex are shown in Figure 4. In their classical

Figure 4. The δ and λ ring conformations of a general ruthenium-amino alcohol complex.

analysis, Corey and Bailar showed that because of this puckering the substituents at the carbons of an ethylenediamine ligand become equatorial and axial.[36] The same differentiation of the carbon substituents is brought about by the puckering in the five-membered rings of the ruthenium amino alcohol complexes. When the amino alcohol ligand in catalyst **2** is coordinated in a δ conformation, the methyl substituent is oriented in an equatorial fashion, whereas in the λ conformation the methyl substituent is oriented in an axial fashion.

Since the ruthenium atom is chiral, two different diastereomeric complexes, (R_{Ru},S_C) and (S_{Ru},S_C), can be formed upon complexation of the metal precursor and the ligand.

Four structures were calculated for each ligand, each diastereomeric complex contained a ligand in the δ or λ conformation. According to the calculations, the differences in calculated energies are relatively small. It should be noted that the calculations are accurate within a few kcal mol^{-1}. Table 6 shows that the (S_{Ru},S_C) diastereomer gives rise to the most stable complex for both ligands and ring conformations. Usually, complexes in which the ligand substituents adopt equatorial arrangements are more stable than the corresponding axially arranged complexes. The calculated relative energies in Table 6 show, however, that this is only the case for the (S_{Ru},S_C) diastereomers of **1** and **2**. For the (R_{Ru},S_C) diastereomers of **1** and **2**, the complex in which the methyl group occupies the axial position is calculated to be more stable. The conformation of the ring is determined by the formation of an intramolecular hydrogen bond between the ruthenium hydride and the proton of the amine functionality. The observed intramolecular H ··· H distance is 2.3 Å for the complexes with the lowest relative energies and 2.6 Å for the complexes that are higher in energy. In addition, the dihedral H-Ru-N-H angle is smaller for the complexes with the lowest relative energy. Thus, the complex shows a preference for a planar H-Ru-N-H moiety; this was also found in the intermediates **17**, **17′**, **17**-TS and **17″** in the catalytic cycle of the "hydrogen-bond formation" mechanism. The calculated energy differences between these different conformations are ≈3.5 kcal mol^{-1} (see Table 6). Single-point calculations of the (S_{Ru},S_C)-**2**-δ and (S_{Ru},S_C)-**2**-λ complexes, in which the methyl substituents were omitted, showed that the energy difference between the δ and λ ring conformations for this unsubstituted amino alcohol complex is only 2.5 kcal mol^{-1}. The additional difference of 1.0 kcal mol^{-1} results from the methyl substituent in the ring. Additional substituents in the amino alcohol backbone will result in a more rigid catalyst and will almost certainly decrease or even prevent the inversion of the ring conformations, as was also indicated by Brunner and coworkers.[37]

The eight possible conformations of catalysts **1** and **2** are depicted in Figure 5. Table 6 shows that the (S_{Ru},S_C)-**1**-δ and the (S_{Ru},S_C)-**2**-δ conformations are the lowest in calculated relative energies, although the differences are small.

As was shown for intermediates **17**-TS, **17′** and **17″** (Table 3 and Figure 1), the dihedral H-Ru-N-H angle in the six-membered ring should be small in order to transfer a proton and a hydride from the catalyst to the substrate. This suggests that the most relevant conformation for the (S_{Ru},S_C) diastereomers is the δ conformation, whereas the λ conformation is the most relevant for the (R_{Ru},S_C) diastereomers. NMR studies of the in situ generated catalyst indicated the presence of the two diastereomers in a 1:2 ratio. Only one ring conformation is observed in the NMR spectrum. The interconversion of the λ and δ ring conformations is either too fast to observe on the NMR time scale or only one conformation is present in solution.

Attempts to rationalise the observed chiral induction effects: In the following we qualitatively combine the experimental results and the results of the quantum mechanical calculations of intermediates **16**–**18** and complexes **1** and **2** in order to gain a more complete understanding of the catalytic reaction. Asymmetric catalysis is a challenge to theoretical investigations because it is sensitive to energy differences of less than 1 kcal mol^{-1}.[38] Various theoretical studies on the origin of enantioselectivity have been performed by the use of different calculation methods, such as QM/MM and density functional theory.[39–47]

In order to rationalise the marked difference in enantioselection between catalysts **1** and **2**, it is necessary to take a closer look at the step which determines the enantioselectiv-

0947-6539/00/0615-2826 $ 17.50+.50/0 *Chem. Eur. J.* **2000**, *6*, No. 15

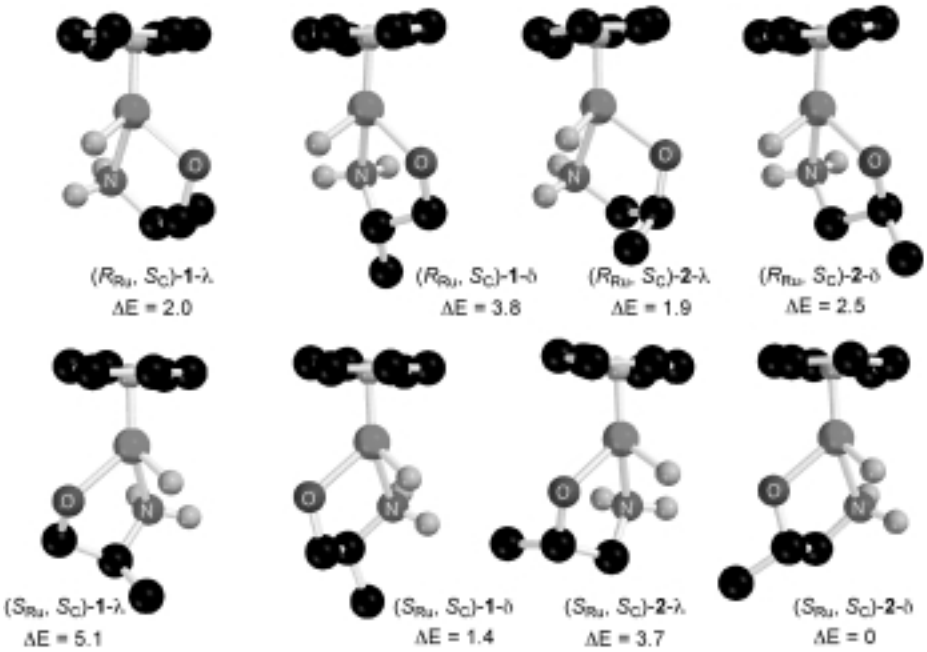

Figure 5. Eight different conformations for **1** and **2**. The hydrogen atoms on the carbon and oxygen atoms have been omitted for clarity.

ity. From the calculations of intermediates **16**–**18** it is clear that the way the ketone approaches the ruthenium-amino alcohol complex, as in intermediates **17″**, **17′** and **17**-TS, determines the enantioselectivity of the reaction. The position of the substituents of the ketone in relation to the amino alcohol ligand is highly important in this series of steps. The ketone substrate will approach the ruthenium complex in such a way that it will be able to form both a hydrogen bond between the proton of the amine and the lone pair electrons of the carbonyl and a bond between the carbonyl carbon and the ruthenium hydride (see Figure 1). The chiral information present in the catalyst will differentiate between the *re* face and the *si* face of the ketone substrate.

In order to visualise these interactions, the structure of formaldehyde complexed to (S_{Ru},S_C)-**2**-δ was calculated similarly to **17′** with ADF and the PW91 functional.[27] In order to visualise the steric interactions, one of the protons of formaldehyde was substituted by a phenyl group, as in acetophenone (see Figure 6). The formation of a hydrogen

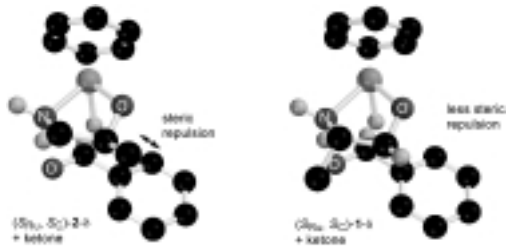

Figure 6. Unfavourable ketone approach towards catalysts **2** and **1**.

bond between the amine proton and the carbonyl oxygen is proved by the short distance of 1.6 Å. Moreover, the ruthenium hydride is positioned close (i.e. 1.3 Å) to the carbonyl carbon which is necessary to obtain the alcoholic product. One of the substituents of the ketone points backwards, whereas the other substituent points towards the methyl substituent in the amino alcohol ligand in **2**.

It is clear that the *re* approach is not sterically hindered for either catalyst **1** or catalyst **2**, since the phenyl group points away from the complex. The enantioselectivity is thus determined by a hindered approach of the ketone at the *si* face of the molecule. Figure 6 shows that the methyl group in catalyst **2** is much closer to the phenyl group of the substrate than the methyl group in catalyst **1**. This explains the higher enantioselectivity towards the (*S*) product obtained by catalyst **2**.

It can be seen from Table 2 that the substitution of the amine functionality in the amino alcohol ligand further improves the enantioselectivity of the transfer hydrogenation of acetophenone to a large extent. The two possible structures for (S_{Ru},S_C)-*N*(Me)-1-amino-2-propanol are depicted in Figure 7. Since a short intramolecular

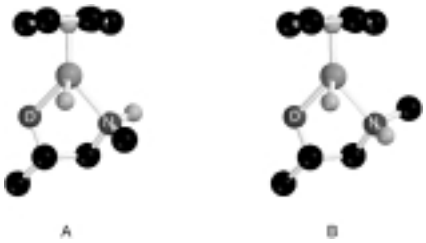

Figure 7. Two possible isomers for (S_{Ru},S_C)-*N*-Me-1-amino-2-propanol, calculated by single-point calculations and starting from (S_{Ru},S_C)-**2**-δ. The hydrogen atoms on the carbon and oxygen atoms have been omitted for clarity.

H···H distance and a small dihedral H-Ru-N-H angle give rise to low relative energies, isomer A will be less favourable than isomer B. Isomer A will most likely result in an inactive catalyst since it is unable to form the six-membered ring in the transition state. Isomer B will give rise to a more rigid and bulky complex compared to the unsubstituted amino alcohol ligand. It has been suggested that more rigid complexes will give rise to a decrease in the inversion of the δ and λ ring conformations which might be the reason for the higher enantioselectivities.[34] These rigid complexes can stabilise the conformation of the complex with the small H-Ru-N-H dihedral angle, and thus the transition state structure.

It should be noted, however, that steric interactions between a bulky substituent at the 2-position of the amino alcohol ligand and a substituent at the amine functionality might prevent the formation of the desired isomer B. Possible

  0947-6539/00/0615-2827 $ 17.50+.50/0

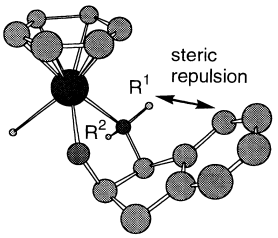

Figure 8. Calculated structure of [RuH{(1*R*,2*S*)-2-amino indanol}{benzene}]. The hydrogen atoms on the carbon and oxygen atoms have been omitted for clarity.

examples of such ligands are (1*R*,2*S*)-2-amino-indanol[3] or the *erythro* series of *N*-substituted (1*S*,2*R*)-2-amino-1,2-diphenylethanols.[2, 5] Preliminary calculations of the ruthenium complexes containing these two ligands showed a steric interaction between the R^1 position on the amine and the phenyl group of the ligand, as is visualised in Figure 8. In this case the substituent at the amine functionality can be positioned as in isomer A, which will most likely result in low catalyst activities, as is observed experimentally.

Conclusions

A systematic investigation of the factors that affect the enantioselective outcome of ruthenium(II) amino alcohol catalysed transfer hydrogenation allowed the determination of a ligand structure – enantioselectivity relationship. It was shown that the substituent at the 1-position of the amino alcohol determines the product configuration, whereas further optimisation of the ligand structure is most effective at the amine functionality and on the arene ring. In order to obtain high asymmetric inductions, a three-dimensional framework around the metal centre, obtained by cooperative steric interactions, is essential.

DFT calculations on the intermediates of the two proposed mechanisms showed that the "hydrogen-bond formation" mechanism, as proposed by Noyori and co-workers, is clearly the most favourable pathway for the transfer of a hydride to the ketone substrate. This is in agreement with the observed low activity for Ru^{II} amino alcohol catalysts that contain a tertiary amine functionality. The migratory insertion mechanism is calculated to go either via intermediates with a high energy or via intermediates that are not in agreement with the experimental data.

The calculations show that the formation of a small intramolecular H···H distance and a planar H-Ru-N-H moiety will lead to stabilisation of the complex. The transition state of the hydrogen-transfer reactions proves to be stabilised by the same factors.

DFT calculations on the putative acetophenone adducts of the two key catalysts were performed in an attempt to rationalise the observed enantioselectivities. These calculations indicated that the enantiodifferentiation in (S_{Ru},S_C)-**2**-δ is most likely higher than in (S_{Ru},S_C)-**1**-δ, in accordance with the experiments. While inaccuracies of the method may not allow firm conclusions, the computer graphics strongly suggests that substitution at C1 is indeed more effective than substitution at C2. As yet, very accurate calculations are not available and the effects of solvation and entropy should be included to arrive at a detailed explanation.

Experimental Section

General remarks: Reactions were carried out in anhydrous solvents under an atmosphere of argon in flame-dried Schlenk flasks. Propan-2-ol was freshly distilled from CaH_2 prior to use. ^1H NMR spectra were recorded on a Varian 300 spectrometer. Chemical shifts are in ppm relative to TMS as the internal standard. Gas chromatography was performed on a Carlo Erba GC 6000 Vega 2 instrument, 25 m column: CycloSil-B (chiral) and a Carlo Erba HRGC Mega 2 instrument, 25 m column: BPX 35 (SGE) (achiral).

Enantioselective reduction of ketones: A solution of the (arene)ruthenium(II) chloride dimer (0.0125 mmol) and the amino alcohol (0.03 mmol) in dry propan-2-ol (5 mL) was heated at 80 °C for 1 h under argon. After cooling the mixture to room temperature, it was diluted with propan-2-ol (43.5 mL) and *t*BuOK (1.5 mL, 0.1 M in propan-2-ol, 0.15 mmol) and the ketone (5 mmol) was added. The reaction was carried out at room temperature under argon for the time given in Table 2 and monitored by GC.

Acknowledgements

The Innovation Oriented Research Programme (IOP-Katalyse) is acknowledged for their financial support of this research. J.-W.H. acknowledges NWO-CW (Nederlandse Organisatie voor Wetenschappelijk Onderzoek, Chemische Wetenschappen) and E.J.M. the Royal Netherlands Academy of Arts and Sciences for financial support. The authors would like to thank Prof. Dr H. Berke, Dr S. Sabo-Etienne and Prof. Dr M. Etienne for fruitful discussions.

[1] R. Noyori, Asymmetric Catalysis in Organic Synthesis, Wiley, New York, **1994**, Chapter 2.
[2] J. Takehara, S. Hashiguchi, A. Fujii, I. Shin-ichi, T. Ikariya, R. Noyori, *Chem. Commun.* **1996**, 233 – 234.
[3] a) M. Palmer, T. Walsgrove, M. Wills, *J. Org. Chem.* **1997**, *62*, 5226 – 5228; b) A. J. Blacker, B. J. Mellor (Zeneca), WO 98/42643 A1, **1998**.
[4] a) D. A. Alonso, D. Guijarro, P. Pinho, O. Temme, P. G. Andersson, *J. Org. Chem.* **1998**, *63*, 2749 – 2751; b) After the submission of this manuscript a follow-up of this paper appeared, which describes theoretical studies on the mechanism of the reaction that are similar to ours: D. A. Alonso, P. Brandt, S. J. M. Nordin, P. G. Andersson, *J. Am. Chem. Soc.* **1999**, *121*, 9580 – 9588.
[5] D. G. I. Petra, P. C. J. Kamer, P. W. N. M. van Leeuwen, K. Goubitz, A. M. van Loon, J. G. de Vries, H. E. Schoemaker, *Eur. J. Inorg. Chem.* **1999**, *12*, 2335.
[6] G. Zassinovich, G. Mestroni, *Chem. Rev.* **1992**, *92*, 1051.
[7] K.-J. Haack, S. Hashiguchi, A. Fujii, T. Ikariya, R. Noyori, *Angew. Chem.* **1997**, *109*, 297 – 300; *Angew. Chem. Int. Ed. Engl.* **1997**, *36*, 285 – 288.
[8] P. Zandbergen, A. M. C. H. van den Nieuwendijk, J. Brussee, A. van der Gen, C. G. Kruse, *Tetrahedron* **1992**, *48*, 3977 – 3982.
[9] S. Hashiguchi, A. Fujii, J. Takehara, T. Ikariya, R. Noyori, *J. Am. Chem. Soc.* **1995**, *117*, 1441 – 1446.
[10] R. Noyori, S. Hashiguchi, *Acc. Chem. Res.* **1997**, *30*, 97 – 102.
[11] A. Aranyos, G. Csjernyik, K. J. Szabó, J.-E. Bäckvall, *Chem. Commun.* **1999**, 351 – 352.
[12] M. Bernard, V. Guiral, F. Delbecq, F. Fache, P. Sautet, M. Lemaire, *J. Am. Chem. Soc.* **1998**, *120*, 1441 – 1446.
[13] V. Rodriguez, S. Sabo-Ettiene, B. Chaudret, J. Thoburn, S. Ulrich, H.-H. Limbach, J. Eckert, J.-C. Barthelat, K. Hussein, C. J. Marsden, *Inorg. Chem.* **1998**, *37*, 3475 – 3485.
[14] G. Orlova, S. Scheiner, *J. Phys. Chem. A* **1998**, *102*, 4813 – 4818.
[15] G. Orlova, S. Scheiner, T. Kar, *J. Phys. Chem. A* **1999**, *103*, 514 – 520.
[16] Gaussian 98 (Revision A.5), M. J. Frisch, G. W. Trucks, H. B. Schlegel, G. E. Scuseria, M. A. Robb, J. R. Cheeseman, V. G. Zakrzewski, J. A. Montgomery, R. E. Stratmann, J. C. Burant, S. Dapprich, J. M. Millam, A. D. Daniels, K. N. Kudin, M. C. Strain, O. Farkas, J. Tomasi, V. Barone, M. Cossi, R. Cammi, B. Mennucci, C. Pomelli, C. Adamo, S. Clifford, J.Ochterski, G. A. Petersson, P. Y. Ayala, Q. Cui, K. Morokuma, D. K. Malick, A. D. Rabuck, K. Raghavachari, J. B.

  0947-6539/00/0615-2828 $ 17.50+.50/0

Foresman, J. Cioslowski, J. V. Ortiz, B. B. Stefanov, G. Liu, A. Liashenko, P. Piskorz, I. Komaromi, R. Gomperts, R. L. Martin, D. J. Fox, , T. Keith, M. A. Al-Laham, C. Y. Peng, A. Nanayakkara, C. Gonzalez, M. Challacombe, P. M. W. Gill, B. G. Johnson, W. Chen, M. W. Wong, J. L. Andres, M. Head-Gordon, E. S. Replogle, J. A. Pople, Gaussian, Inc., Pittsburgh, PA, **1998**.

[17] ADF, **1999**, Theoretical Chemistry; Vrije Universiteit Amsterdam (The Netherlands). Contributers: E. J. Baerends, A. Bérces, C. Bo, P. M. Boerrigter, L. Cavallo, L. Deng, R. M. Dickson, D. E. Ellis, L. Fan, T. H. Fischer, C. Fonseca Guerra, S. J. A. van Gisbergen, J. A. Groeneveld, O. V. Gritsenko, F. E. Harris, P. van den Hoek, H. Jacobsen, G. van Kessel, F. Kootstra, E. van Lenthe, V. P. Osinga, P. H. T. Philipsen, D. Post, C. C. Pye, W. Ravenek, P. Ros, P. R. T. Schipper, G. Schreckenbach, J. G. Snijders, M. Sola, D. Swerhone, G. te Velde, P. Vernooijs, L. Versluis, O. Visser, E. van Wezenbeek, G. Wiesenekker, S. K. Wolff, T. K. Woo, T. Ziegler.

[18] C. Fonseca Guerra, J. G. Snijders, G. te Velde, E. J. Baerends, *Theor. Chem. Acc.* **1998**, *99*, 391.

[19] A. D. Becke, *Phys. Rev. A.* **1988**, *38* , 3098.

[20] J. P. Perdew, J. A. Chevary, S. H. Vosko, K. A. Jackson, M. R. Pederson, D. J. Singh, C. Fiolhais, *Phys. Rev. B* **1992**, *46*, 6671.

[21] T. H. Dunning, P. J. Hay, *Modern Theoretical Chemistry*, Plenum, New York, **1977**, *3*, 1.

[22] P. J. Hay, W. R. Wadt, *J. Chem. Phys.* **1985**, *82*, 270, 299.

[23] S. H. Vosko, L. Wilk, M. Nusair, *Can. J. Phys.* **1980**, *58*, 1200.

[24] C. Lee, W. Yang, R. G. Parr, *Phys. Rev. B* **1988**, *37*, 785.

[25] Molecular orbitals were expanded by means of the LANL2DZ basis set.

[26] Molecular orbitals were expanded in an uncontracted triple δ Slater-type basis set augmented with 2p and 3d polarisation functions for H, 3d and 4f polarisation functions for C, N, and O. No polarisation functions were added for Ru. The cores were kept frozen.

[27] A. D. Becke, *J. Chem. Phys.* **1993**, *98*, 5648–5652.

[28] B. Miechlish, A. Savin, H. Stoll, H. Preuss, *Chem. Phys. Lett.* **1989**, *157*, 200.

[29] G. Orlova, S. Scheiner, *J. Phys. Chem. A* **1998**, *102*, 260.

[30] V. Jonas, W. J. Thiel, *Chem. Phys.* **1996**, *105*, 3636.

[31] V. Jonas, W. J. Thiel, *Chem. Phys.* **1995**, *102*, 8474.

[32] I. Bytheway, G. B. Bacskay, N. S. Hush, *J. Phys. Chem.* **1996**, *100*, 6023.

[33] I. Bytheway, G. B. Bacskay, N. S. Hush, *J. Phys. Chem.* **1996**, *100*, 14899.

[34] It should be noted that all the relative energies of the intermediates were calculated in the gas phase. In solution, compounds **16** and **18** will also be stabilised by the formation of hydrogen bonds to the solvent.

[35] We would like to acknowledge one of the referees for this useful suggestion.

[36] E. J. Corey, J. C. Bailer, Jr, *J. Am. Chem. Soc.* **1959**, *81*, 2620.

[37] H. Brunner, *J. Organometal. Chem.* **1986**, *300*, 39–56, and references therein.

[38] P. E. Blöchl, A. Togni, *Organometallics* **1996**, *15*, 4125–4132.

[39] K. V. Gothelf, R. G. Hazell, K. A. Jorgensen, *J. Org. Chem.* **1996**, *61*, 346–355.

[40] G. Ujaque, F. Maderas, A. Lledos, *Theor. Chim. Acta* **1996**, *94*, 67–73.

[41] F. Agbossou, J. F. Carpentier, A. Mortreux, G. Surpateanu, A. J. Welch, *New J. Chem.* **1996**, *20*, 1047–1060.

[42] P. H. Hunenberger, J. K. Granwehr, J. N. Aebischer, N. Ghoneim, E. Haselbach, W. F. van Gunsteren, *J. Am. Chem. Soc.* **1997**, *119*, 7533–7544.

[43] G. Colombo, G. Ottolina, G. Carrea, A. Bernardi, C. Scolastico, *Tetrahedron Asymmetry* **1998**, *9*, 1205–1214.

[44] G. Surpateanu, F. Agbossou, J. F. Carpentier, A. Mortreux, *Tetrahedron Asymmetry* **1998**, *9*, 2259–2270.

[45] M. Sundaramoorthy, J. Terner, T. L. Poulos, *Chem. Biol.* **1998**, *5*, 461–473.

[46] G. Ujaque, F. Maseras, A. Lledos, *J. Am. Chem. Soc.* **1999**, *121*, 1317–1323.

[47] M. Yamakawa, R. Noyori, *Organometallics* **1999**, *18*, 128–133.

Received: October 14, 1999 [F2091]